Physical gels from PVC: dynamic properties of dilute solutions

S. J. Candau and Y. Dormoy
Laboratoire de Spectrométrie et d'Imagerie Ultrasonores, Unité Associée au CNRS, Université Louis Pasteur, 4, rue Blaise Pascal, 67070 Strasbourg Cédex, France

and P. H. Mutin, F. Debeauvais and J. M. Guenet
Institut Charles Sadron (CRM-EAHP), CNRS/ULP, 6, rue Boussingault, 67083 Strasbourg Cédex, France
(Received 19 May 1986; revised 23 September 1986; accepted 29 October 1986)

In an effort to gain information on the gelation mechanism of poly(vinyl chloride) (PVC) in diethyl malonate, investigations of dilute PVC solutions were made using transient electric birefringence, flow birefringence, dynamic light scattering and viscometry. The dynamical structure factor obtained from the cumulant analysis of the autocorrelation function of scattered field exhibits an anomalous K dependence which can be attributed to an intramolecular effect. Measurements of intrinsic viscosity and rotational diffusion coefficient provide information on the internal structure of the aggregates formed by quenching dilute PVC solutions.

(Keywords: poly(vinyl chloride); physical gels; transient electric birefringence; flow birefringence; light scattering; photon correlation spectroscopy)

INTRODUCTION

The mechanism of physical gelation of PVC solutions is still open to discussion and thereby remains a topical issue. Hitherto, two major models have been proposed that are totally different as long as the early stage of gelation is involved.

On one hand, it is thought[1] that some stereoregular syndiotactic sequences of the chains crystallize leading to the formation of tiny crystals of a fringed-micellar type responsible for interchain bridging. On the other hand, Yang and Geil[2] claim, on the basis of d.s.c. experiments, that, although crystals may grow on ageing, the early stage of gelation does not involve crystallization since the melting endotherm appears only several hours after the gel is formed. They therefore suggest that gelation arises from hydrogen bondings between chains and correspondingly that the junctions are rather punctual. These conflicting conclusions are inherent to the difficulties encountered in the investigation of systems out of equilibrium, characterized by ageing effects. These effects are drastically reduced in small aggregates formed by quenching dilute PVC solutions. Recent light scattering experiments carried out on dilute PVC solutions in linear esters have given strong evidence for the presence of optically inhomogeneous crosslinked particles[3].

The purpose of this paper is to investigate these dilute solutions by means of several techniques sensitive to the hydrodynamic properties: transient electric birefringence, flow birefringence, quasi-elastic light scattering and viscometry. These experiments provide further information on the structure of the aggregates and of the junctions between chains.

EXPERIMENTAL

Materials

A PVC of commercial origin (Rhone-Poulenc S.A.) was used without further purification. This polymer has been synthesized at 50°C and is therefore mainly atactic. Tacticity characterization by ^{13}C n.m.r. in cyclohexanone solutions has given the following ratio for the syndiotactic (s), heterotactic (h) and isotactic (i) triades:

$$s = 0.33 \qquad h = 0.49 \qquad i = 0.18$$

Molecular weight determinations were achieved using g.p.c. in THF at room temperature giving $M_w = 1.2 \times 10^5$ and $M_w/M_n = 2.3$. The g.p.c. columns were calibrated using standard polystyrene fractions. Freshly distilled diethylmalonate (DEM) was used as a solvent.

Sample preparation

A solution at a concentration $C_s = 0.5 \times 10^{-2}$ g cm^{-3} was prepared under vigorous stirring at 150°C and then cooled to 23°C. It was checked by n.m.r. and infra-red spectroscopy that no alteration nor chemical modification had occurred[3]. After quenching, the solution was allowed to stand at room temperature for three days and then diluted at the required concentrations.

Transient electric birefringence

A He–Ne laser beam, ($\lambda = 632.8$ nm) was polarized at $3\pi/4$ to the vertical and propagated parallel to the surface of two vertical flat 'inox' electrodes immersed in the solution being studied. The spacing between the electrodes was 2.5 mm and their length 40 mm. High

0032-3861/87/081334-07$03.00

voltage rectangular pulses were applied to the electrodes, of variable duration (from 10 μs to 10 ms, rise and decay times $< 0.2\,\mu$s) and variable amplitude (up to 500 V for a single pulse and 250 V for a sequence of a positive pulse and a negative pulse). The inversion of the field takes place in less than 1 μs. As the decay time of the negative pulse, due to generator limitation is $\simeq 10\,\mu$s, birefringence decay times have only been measured after positive pulse excitation. The light beam emerging from the Kerr cell passes through a quarter wave plate whose slow axis at $3\pi/4$ is parallel to the polarization direction, and through an analyser, before detection with a photodiode. The output signal was sampled with a transient DATALAB DL 922 recorder (8 bits, 2048 channels memory, 20 MHz maximum sampling rate) together with the high voltage electric pulse applied to the cell. The digital signals were sent to a HP 86 computer to be processed. Several recordings for each experimental condition were stored for further analysis.

Flow birefringence measurements

The flow birefringence experiments were performed using a high-sensitivity apparatus; the incident light beam was modulated by a rotating crystal synchronized with the photoelectric detection. The temperature was regulated both inside and outside the flow-cell. The temperature gradient between the walls was less than 0.004°C. The internal rotor was 50 mm in diameter, 70 mm in length and with a 0.5 mm gap. The speed of rotation of the internal cylinder determines the shear rate G in the gap and the magnitude of the flow birefringence Δn. The procedure for obtaining the orientation angle ϕ of the polarization ellipse and of the birefringence are fully described elsewhere[4]. The birefringence was measured using a null-method which permitted the elimination of all spurious birefringence effects.

Viscometry

A Sofica automatic capillary viscometer with a capillary diameter 0.6 mm was used. The viscosities were measured at $T = 25$°C.

Correlation time measurements

Experiments were performed by using either an argon ion laser ($\lambda = 488$ nm) or a helium–neon laser ($\lambda = 632.8$ nm) in conjunction with a 72 channel clipped digital autocorrelator for measuring the autocorrelation function of the scattered light intensity in the homodyne regime. The scattering angle was varied from 15° to 135°. The temperature was held constant to within ± 0.01°C.

Intensity correlation data were routinely processed, using the cumulants method to provide the average decay rate $\langle\Gamma\rangle$ and the reduced variance v[5,6]. The latter parameter is a measure of the width of the distribution of decay rates and is given by:

$$v = (\langle\Gamma^2\rangle - \langle\Gamma\rangle^2)/\langle\Gamma\rangle^2 \tag{1}$$

In the case of homogeneous particles the diffusion coefficient D is given by the first reduced cumulant $\langle\Gamma\rangle/2K^2$. The magnitude of the scattering vector K is given by:

$$K = [4\pi n \sin(\theta/2)]/\lambda \tag{2}$$

where θ is the scattering angle, λ is the wavelength of the incident light in a vacuum and n is the refractive index of the scattering medium.

EXPERIMENTAL RESULTS

Transient electric birefringence

Figure 1 shows the time dependence of the birefringence $\Delta n(t)$ induced by applying successively a positive and a negative electric field pulse to a solution of PVC at $c = 10^{-3}$ g cm^{-3}.

In the general case where rigid revolution ellipsoidal particles in solution possess both a permanent and an induced dipolar moment collinear with the partial optical axis, the theory derived by Tinoco predicts the following behaviour of $\Delta n(t)$ in the limit of the weak electric field[7]:

(a) The rise of birefringence following the setting-up of the electric field is given by:

$$\Delta n(t) = \Delta n_0\left[1 - \frac{3P/Q}{2(P/Q+1)}e^{-2D_R t} + \frac{P/Q-2}{2(P/Q+1)}e^{-6D_R t}\right] \tag{3}$$

where Δn_0 is the value of the steady-state birefringence, D_R is the rotational diffusion constant of the particle and:

$$P = \mu^2/k_B^2 T^2$$
$$Q = (\alpha_1 - \alpha_2)/k_B T \tag{4}$$

where μ is the permanent dipolar moment and α_1 and α_2 are the electrical polarizabilities of the particle parallel and perpendicular to the revolution axis, respectively. k_B is the Boltzmann constant and T is the absolute temperature.

(b) The transient regime, following the inversion of electric field, is described by:

$$\Delta n(t) = \Delta n_0 + \Delta n_0\left(\frac{3P/Q}{P/Q+1}\right)(e^{-6D_R t} - e^{-2D_R t}) \tag{5}$$

If the particle does not possess any permanent dipole ($P/Q = 0$) the birefringence remains stationary upon field inversion. If there is a contribution from the permanent dipole, then Δn reaches a minimum Δn_{min} related to P/Q according to:

$$\frac{P}{Q} = \frac{1 - \dfrac{\Delta n_{min}}{\Delta n_0}}{0.1547 + \dfrac{\Delta n_{min}}{\Delta n_0}} \tag{6}$$

This minimum occurs at a time t_{min} given by:

$$t_{min} = 0.2747\, D_R^{-1} \tag{7}$$

The birefringence decay following rempval of the field is exponential according to[8]:

$$\Delta n(t) = \Delta n_0 e^{-6D_R t} \tag{8}$$

Inspection of *Figure 1* shows that the PVC particles possess a permanent dipole moment.

The theoretical curve described by equation (5) is fitted

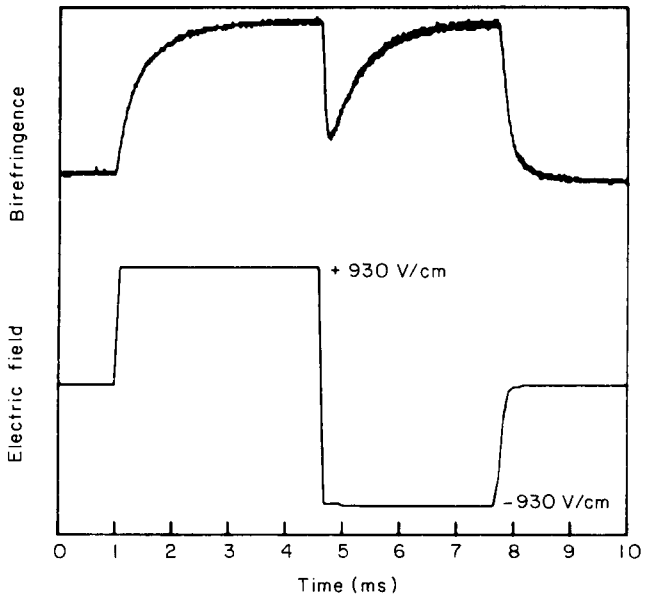

Figure 1 Time dependence of the output photodiode signal proportional to the electric birefringence. $c = 10^{-3}\,g\,cm^{-3}$, $T = 23°C$. The best fits to equations (3) and (8) are indistinguishable from the experimental curves

to the experimental rise curve of the birefringence where the agreement is found to be reasonably good with the rotational diffusion constant D_R and the P/Q ratio obtained from the best fit being:

$$D_R = 1.33 \times 10^3 \pm 0.1 \times 10^3\,s^{-1}$$

$$\frac{P}{Q} = 1.81 \pm 0.1$$

From the value of t_{min} and Δn_{min} measured on reversing of the electric pulse, and using equations (6) and (7) we obtain:

$$D_R = 1.88 \times 10^3 \pm 0.5 \times 10^3\,s^{-1}$$

$$\frac{P}{Q} = 1.82 \pm 0.1$$

A single exponential curve (equation (8)) is fitted to the decay curve of the birefringence after removal of the electric field. The agreement is also good and this leads to a rotational diffusion constant:

$$D_R = 1.32 \times 10^3 \pm 0.1 \times 10^3\,s^{-1}$$

An analysis of the decay curve with the cumulants method, similar to that used in quasi-elastic light scattering, leads to a slightly better fit; the reduced variance of the distribution is close to 0.14 which denotes a small polydispersity in the particle size. The value of the mean rotational diffusion constant is found to be less than 10% higher than the value deduced from the single exponential fit.

Information concerning absolute values of P and Q are provided by the behaviour of the steady state birefringence Δn_0 *versus* the square of the electric field E; Δn_0 is given by[9]:

$$\frac{\Delta n_0}{\phi} = \frac{2\pi}{n}(g_1 - g_2)\Phi(P/Q, (P+Q)E^2) \qquad (9)$$

where ϕ is the volume fraction of polymer, $(g_1 - g_2)$ the optical anisotropy of the particle, the indices 1 and 2 referring to the revolution and transverse axis, respectively. Φ is the orientation function.

In the limit of weak electric fields equation (9) reduces to:

$$\frac{\Delta n_0}{\phi} = n k_{sp} E^2 \qquad (10)$$

where k_{sp} is the Kerr constant given by:

$$k_{sp} = \frac{2\pi}{15}\frac{g_1 - g_2}{n^2}(P+Q) \qquad (11)$$

Figure 2 shows that the linear variation of Δn_0 *versus* E^2 for the sample is quite linear over the whole electric field range.

Consequently the fit of the equation (9) to the experimental points will not provide precise values for adjustable parameters P, Q and $g_1 - g_2$. If we use the value $P/Q = 1.8$ obtained from the transient behaviour of the birefringence, the best fit of equation (9) to experimental points is then obtained for $P + Q = 1.1 \times 10^{-10}\,m^2/V^2$. This value can be considered as the upper limit of $P + Q$ since the deviation of $\Delta n_0(E^2)$ from linearity is very small and leads to the upper limits of electrical parameters μ and $\alpha_1 - \alpha_2$ as well as the lower limit of $g_1 - g_2$:

$$\mu < 3.5 \times 10^{-26}\,m\,C$$

$$\alpha_1 - \alpha_2 < 1.7 \times 10^{-31}\,F\,m^2$$

$$g_1 - g_2 > 4.4 \times 10^{-6}$$

The specific Kerr constant K_{sp} is, whatever P/Q:

$$K_{sp} = 1.1 \times 10^{-16}\,m^2/V^2$$

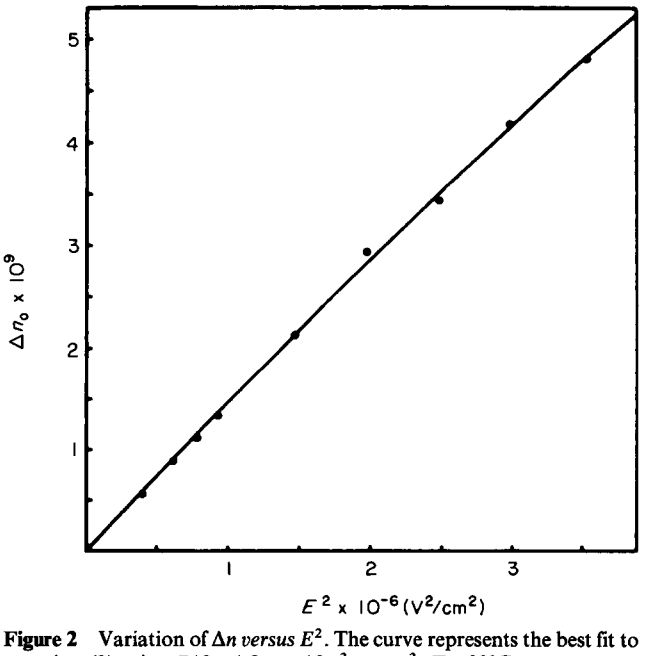

Figure 2 Variation of Δn *versus* E^2. The curve represents the best fit to equation (9) using $P/Q = 1.8$, $c = 10^{-3}\,g\,cm^{-3}$, $T = 23°C$

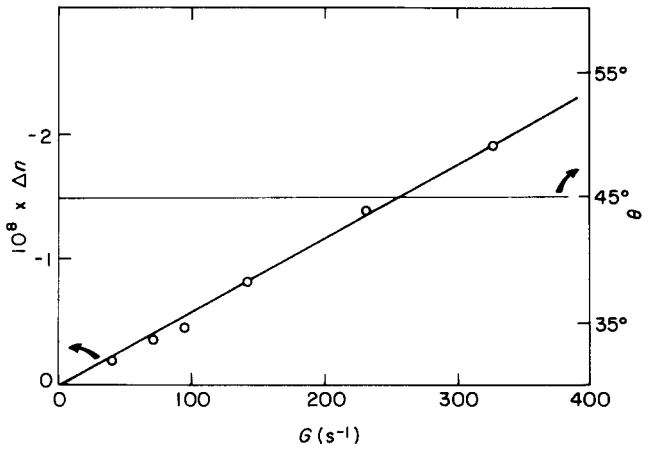

Figure 3 Variations of the flow birefringence and the orientation angle *versus* the velocity gradient, $c = 10^{-3}\,g\,cm^{-3}$, $T = 23°C$

Flow birefringence

The flow birefringence was found to be negative and proportional to the velocity gradient (see *Figure 3*). This last result indicates that the PVC solutions exhibit Newtonian behaviour, in agreement with the viscometric experiments. Moreover the orientation angle of the polarization ellipse was equal to 45°, whatever the shear rate and the PVC concentration (in the range 10^{-3}–$5 \times 10^{-3}\,g\,cm^{-3}$). This result differs from those found for linear polymer solutions where the orientation angle usually decreases upon increasing G[10].

The following concentration dependence of $\Delta n/G$ is found:

$$\frac{\Delta n}{G\eta_0}(s\,P^{-1}) = -3.2 \times 10^{-6} c\,(g\,cm^{-3})$$

The viscosity of the solvent η_0 is equal to 0.02 P.

The above behaviour is characteristic of a deformation rather than an orientation of the particle and can be described by the elastic sphere model derived by Cerf[11]. This model predicts for the angle θ of the polarization ellipse the following expression

$$\theta = \frac{\pi}{4} + \frac{1.25}{\mu_s}\eta_0 \qquad (12)$$

where μ_s is the shear modulus of the particle and the internal viscosity effects have been neglected. In the limit of high shear modulus $\theta = \pi/4$, a value observed here.

Assuming that the polarizability ellipsoid of the particle and the strain ellipsoid have the same main directions, the model predicts the following expression for the birefringence:

$$\frac{1}{n_0\eta_0}\left(\frac{\Delta n}{cG}\right) \simeq \frac{1}{\eta_0^2\mu_s}\left[5\alpha + 2\left(\frac{\delta n}{n}\right)^2\right] \qquad (13)$$

where α is a proportionality constant between the relative variations of the refractive index and the strain components along the main deformation axis; δn is the difference between the refractive indices n of the particle and n_0 of the solvent.

This equation shows that the birefringence can be negative only if two conditions are simultaneously fulfilled

$$\alpha < 0 \quad \text{and} \quad \left(\frac{\delta n}{n}\right)^2 < \frac{5}{2}\alpha$$

Therefore, the experimentally observed negative birefringence in PVC solutions shows that $\alpha < 0$, which means that the change of polarizability is larger in the direction perpendicular to the deformation.

Viscometry

Figure 4 shows the variation of the specific viscosity $\left(\frac{\eta - \eta_0}{\eta_0 c}\right)$ as a function of PVC concentration. The variation is linear in the range of high dilution.

The intrinsic viscosity obtained from the intercept with the ordinate axis is:

$$[\eta] = \lim_{c \to 0}\left(\frac{\eta - \eta_0}{\eta_0 c}\right) = 26.5 \pm 1\,cm^3\,g^{-1}$$

The slope of the straight line of *Figure 4* is:

$$k'_\eta = 650\,g^{-2}\,cm^6$$

Light scattering

Figure 5 shows the K dependences of the first and the second reduced cumulants for three PVC concentrations. Both $\langle\Gamma\rangle/2K^2$ and v decrease as K increases. Up to now, such a behaviour has been only observed for latex particles of large size (radius > 200 nm) and moderately high volume fraction ($\phi > 10^{-2}$)[12–14]. The amplitude of the variation of $\langle\Gamma\rangle/2K^2$ vs. K has been found to increase with the volume fraction of dispersed particles. The observed behaviour has been attributed to a short-range ordering of the scattering particles and correspondingly, the decrease of the effective diffusion coefficient when going from small to large values of K has been interpreted as a gradual transition from mutual to self-diffusion. Yet, this interpretation is not consistent with our observations of the effect of dilution on scattering properties. This effect is illustrated in *Figure 5* and also in *Figure 6* showing the K dependences of the scattered intensities.

Inspection of *Figures 5* and *6* reveals that there is no detectable effect of concentration. From this observation, one can infer that:

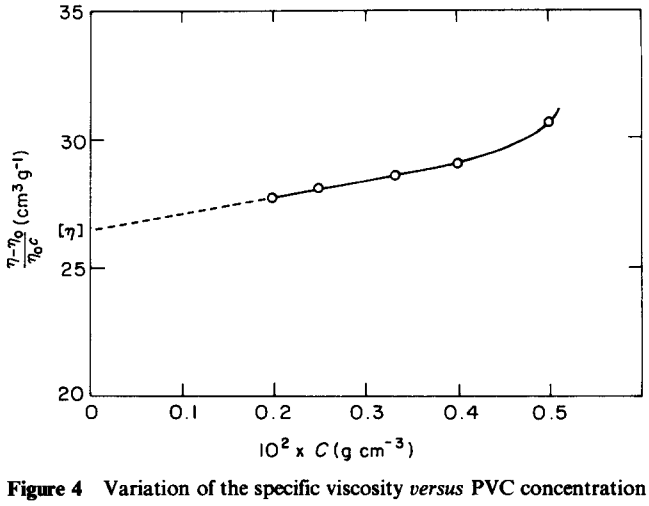

Figure 4 Variation of the specific viscosity *versus* PVC concentration

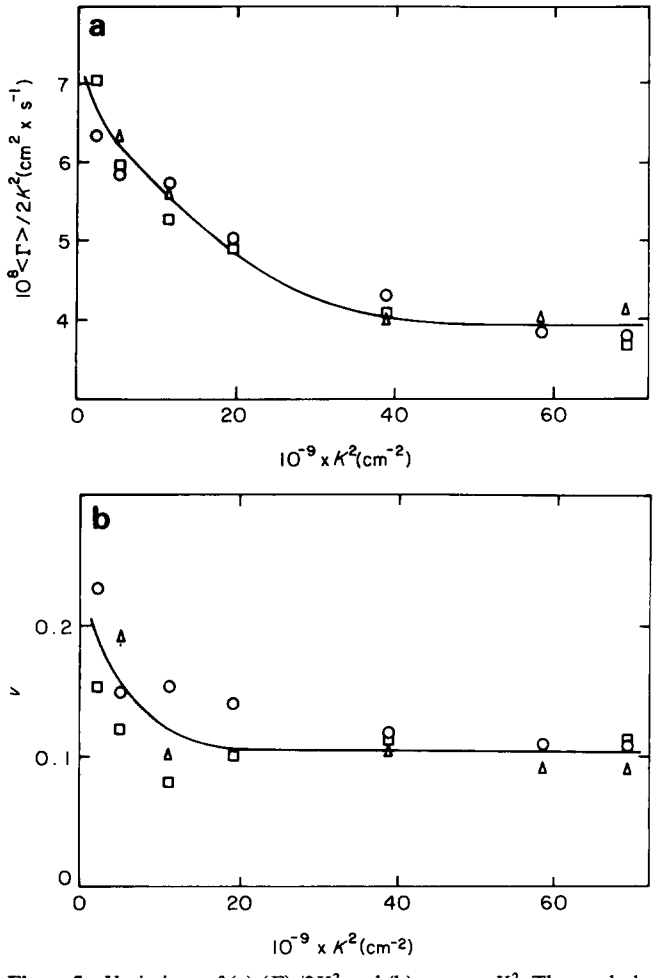

Figure 5 Variations of (a) $\langle\Gamma\rangle/2K^2$ and (b) v *versus* K^2. The symbols refer to concentration (in 10^{-2} g cm^{-3}): 0.5 (○), 0.3 (□), 0.1 (△)

(i) The PVC aggregates formed in the quenching process are stable upon dilution.

(ii) The effect of intermolecular interactions on the first reduced cumulant is negligible. Such behaviour is quite characteristic of highly dispersed hard spheres.

(iii) There is an important anomalous K dependence of $\langle\Gamma\rangle/2K^2$ which could be ascribed to an intramolecular effect.

The anomalous K dependences of the first two cumulants ought to be associated with the shape of the static structure factor obtained from static light scattering data (see *Figure 6*). In this respect, it must be remembered that the cumulant analysis provides, at the limit of high dilution, the following averages of the reduced moments:

$$\langle\Gamma\rangle/2K^2 = \sum_i N_i f_i^2 D_{0i} \Big/ \sum_i N_i f_i^2 \qquad (14)$$

where N_i is the number of particles of species i with diffusion coefficient D_{0i} and scattering amplitude f_i

$$v = \frac{\sum_i N_i f_i^2 D_{0i}^2 \Big/ \sum_i N_i f_i^2}{\left[\sum_i N_i f_i^2 D_{0i} \Big/ \sum_i N_i f_i^2\right]^2} \qquad (15)$$

If the scattered amplitude f_i is a function of K then both $\langle\Gamma\rangle/2K^2$ and v are also K dependent through the polydispersity effect even though the D_{0i}'s are independent of K. Even small polydispersities could produce large effects on the reduced cumulants if $f_i(K)$ is very sensitive to the size and the internal structure of the particles.

DISCUSSION

Shape of the particles

Although there is no unambiguous evidence of the particle shape, there are several observations in favour of a spherical object.

(i) The depolarization ratio of scattered light is almost zero.

(ii) The negative value of the flow birefringence, as well as its proportionality with respect to the shear gradient and the particle concentration, exclude the possibility of elongated particles[10].

(iii) The transient electric birefringence as well as the dynamic light scattering results indicate a small size polydispersity incompatible with anisotropic geometries of the aggregates.

(iv) The proportionality of electric birefringence with the square of the electric field in a large range of values of electric field as well as the small value of the specific Kerr constant excludes the possibility of strong electrical and optical anisotropies.

Size of the particles

Assuming a spherical shape, it is possible to determine an average radius R of the particles from the value of the rotational diffusion constant, using the following relationship:

$$D_R = \frac{k_B T}{8\pi\eta_0 R^3} \qquad (16)$$

For the investigated sample, using the value $D_R = 1.32 \times 10^3$ s^{-1}, obtained from the single exponential fit of the birefringence decay curve, R is found equal to 400 Å.

Swelling of the particles

If one assumes that the PVC aggregates behave, to a first approximation, as swollen spherical particles, impenetrable to the flow, then the viscosity of the solution should obey the equation:

$$\eta = \eta_0(1 + 2.5C_v + k_\eta C_v^2) \qquad (17)$$

where C_v is the volume fraction of dispersed particles, k_η is

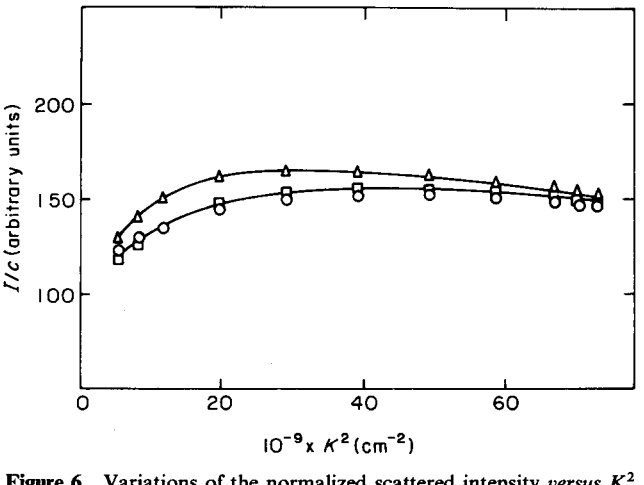

Figure 6 Variations of the normalized scattered intensity *versus* K^2. The symbols refer to concentrations (in 10^{-2} g cm^{-3}): 0.5 (○), 0.3 (□), 0.1 (△)

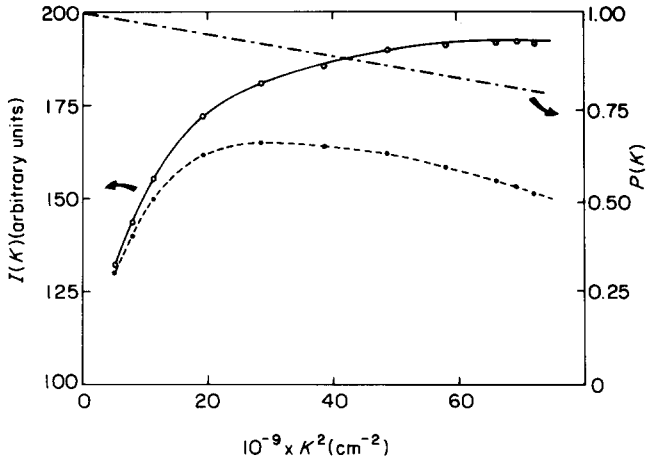

Figure 7 Variation of $S(K)=I(K)/P(K)$ *versus* K^2. $P(K)$ has been calculated from equation (21) with $R=400$ Å; $I(K)$ is the experimental curve for $c=10^{-3}$ g cm^{-3}. (———) $I(K)$; (–·–·–) $P(K)$; (– – –) $S(K)$

an interaction coefficient approximately equal to 4.8[15].

It is convenient to express C_v in terms of the polymer concentration C and the internal concentration C_{int} of these particles (in g cm^{-3})

$$\eta=\eta_0\left[1+2.5\frac{C}{C_{int}}+k_\eta\left(\frac{C}{C_{int}}\right)^2\right] \tag{18}$$

which leads to:

$$[\eta]=\frac{2.5}{C_{int}} \tag{19}$$

From the intercept and the slope of the straight line in *Figure 5* we obtain:

$$C_{int}=9.5\times10^{-2}\text{ g cm}^{-3}, \qquad k_\eta=5.8$$

Combining this value of the internal concentration with the radius obtained from transient electric birefringence we determine an estimate of the molecular weight M of the aggregates

$$M\simeq15\times10^6\text{ g mol}^{-1}$$

which corresponds roughly to a few hundred PVC chains.

Structure of the particles

The static structure factor obtained from the light scattering shows that the crosslinked particles are optically inhomogeneous. The observed behaviour is likely to originate from the presence of crosslinks of crystalline structure.

In this respect we must mention that bell-shaped structure factors have been obtained from small-angle neutron scattering experiments either in polystyrene networks with labelled crosslinks swollen by a hydrogenated solvent, or in *non-labelled* polystyrene networks swollen by a *deuterated* solvent[16].

In the latter case the contrast between crosslinks and chains arises from the high polymer concentration near the crosslinks, involving a low-deuterated solvent concentration.

In PVC aggregates, chains between crosslinks are diluted by the solvent, when solvent molecules cannot enter the crystalline crosslinks. As the refractive indices of PVC and solvent are very different, these concentration inhomogeneities lead to a strong contrast between crosslinks and chains.

Even though the maximum that we observe occurs at lower K values than in neutron experiments, the two phenomena must have similar origins and be associated with intercrosslink correlations. In the present case, we can assume, to a first approximation, that the pattern intensity results from the product of two structure factors $P(K)$ and $S(K)$ associated respectively with the interference factor of a particle assumed to be optically homogeneous and the intercrosslinking interference factor

$$I(K)\sim P(K)\,S(K) \tag{20}$$

Taking for $P(K)$ the expression for a hard sphere[17]

$$P(K)=[3(\sin KR-KR\cos KR)]^2(KR)^{-6} \tag{21}$$

and using for R the value of 400 Å obtained from transient electric birefringence experiments, one obtains the curve represented in *Figure 7*. On the same Figure the variation of $S(K)$ as obtained by dividing the actual $I(K)$ by $P(K)$ is reported. The shape of the resulting curve is quite similar to that theoretically predicted by de Gennes for a bulk of partially labelled chains[18]. This effect, called a 'correlation hole', has been shown theoretically to persist in polymer solutions as long as the chains overlap each other[19]. Although the case presently studied is more complicated because of the excluded volume effects associated with the presence of the crosslinks and the unknown structure of these crosslinks, clearly such a correlation can be considered here.

According to the above considerations, the intensity pattern would depend both on the size of the particles and on the intraparticle spatial distribution of crosslinks. Therefore even a small polydispersity in the particle size and in the spatial distributions of the crosslinks would entail the appearance of particular dynamic structure factor.

The decrease of $\langle\Gamma\rangle/2K^2$ as K increases, observed in *Figure 5* ought to be associated with an interdependence of the internal structure of the aggregates and their size, the contribution of the largest particles to the scattering being reduced in the low K range.

Further information on the nature of the crosslinks is provided by the transient electric birefringence results. The latter have been interpreted assuming a rigid particle orientation theory, taking no account of a possible field induced change of shape of the particle. Indeed, if the electric field orients individual junction zones within the microgel, resulting in particle elastic deformation, one would observe a different behaviour of the birefringence according to the following considerations:

(i) If the deformation rate is faster than the rotational diffusion rate, then, the birefringence rise and decay curves would be symmetrical, which is not the case (*Figure 1*); moreover we should not observe any birefringence decay at the reversing pulse.

(ii) If the deformation rate is longer than the rotational diffusion rate, then the rise curve would be controlled by the deformation process whereas the decay curve would be associated with the rotational diffusion. Indeed the

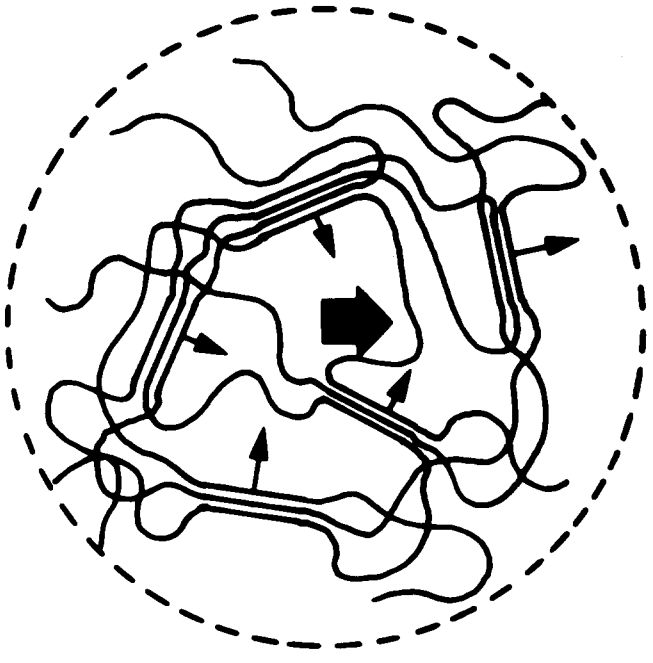

Figure 8 Schematic representation of a PVC aggregate. Small arrows represent the crystallite dipole, the large arrow the resultant dipole in the aggregate

characteristic rise time is approximately three times that of the decay curve, which is what is expected from the rigid particle orientation theory. It could occur coincidentally that the ratio between relaxation times for deformation and orientation be 3. However experiments, which will be reported elsewhere, performed on PVC solutions quenched under different conditions have shown that the ratio 3 was observed irrespective of the particle size provided that the decay curve could be approximated by a single exponential.

Moreover, if a field-induced particle deformation or junction zone orientation occurs, we shall observe, due to the field dependence of the optical anisotropy $(g_1 - g_2)$, large deviation from linearity of the $\Delta n\,(E^2)$ curve.

Therefore the effect of the orientation junction zone is likely to contribute only to the induced dipole and the PVC aggregates must possess a small permanent dipole. This dipole implies the presence of extended chains and the most plausible assumption is that it originates in the C–Cl bonds, perpendicular to the planar zig-zag syndiotactic sequences[20]. Therefore a small crystallite might exhibit a resulting dipole, the strength of which depends on the amount of perfection in the arrangement of the syndiotactic sequences. In the PVC aggregates, there will be a distribution of both orientations and strengths of the dipoles with a non-zero resulting dipole if the number of crosslinks is not too large. A schematic structure of the particle could then be as represented in *Figure 8*. Under an electrical field the particles reorient with a relaxation time associated with the rotational diffusion constant of the particle. The fact that the birefringence is positive indicates that the major axis of the optical polarizability ellipsoid is along the same direction as the permanent dipole, that is perpendicular to the zig-zag chains. This result is in good agreement with stress optical measurements performed in the bulk which show a negative birefringence[21].

The flow birefringence results are also in favour of the structure shown in *Figure 8*. Under shear flow, the PVC aggregates deform in such a way that the chains are elongated along a direction at 45° with respect to the direction of the flow. The resulting birefringence is negative again in accordance with the results obtained in the bulk state.

CONCLUSION

The results presented in this paper show that the quenching of dilute PVC solutions leads to the formation of crosslinked aggregates, stable on dilution. The first reduced cumulant of the autocorrelation function of scattered light exhibits an anomalous K dependence, i.e. a decrease as K increases. This effect is proved to be of intraparticle origin. Hitherto only similar interparticle effects were reported to our knowledge. The observed behaviour is consistent with an optically inhomogeneous structure of physical origin as previously suggested to interpret light scattering data[3]. Transient electric birefringence experiments show that the aggregates exhibit a permanent dipole and correlatively an optical anisotropy, which we assumed to be associated with crosslinks made of small syndiotactic crystallites. A detailed investigation of the thermal stability of the PVC aggregates as a function of the concentration at which they are quenched will be presented in a subsequent paper.

ACKNOWLEDGEMENTS

We are very much indebted to H. Benoit, L. Leibler and R. Cerf for useful discussions. One of us (P.H.M.) thanks 'Rhovyl S.A.' for financial support.

REFERENCES

1 Guerrero, S. J. and Keller, A. *J. Polym. Sci., Polym. Phys. Edn.* 1980, **18**, 1533
2 Yang, Y. S. and Geil, P. H. *J. Macromol. Sci. Phys.* 1983, **B22(3)**, 463
3 Mutin, P. H. and Guenet, J. M. *Polymer* 1986, **27**, 1098
4 Picot, C. and Debeauvais, F. *Polym. Eng. Sci.* 1975, **15**, 373
5 Koppel, D. E. *J. Chem. Phys.* 1972, **57**, 4814
6 Brown, J. C., Pusey, P. N. and Dietz, R. J. *J. Chem. Phys.* 1975, **62**, 1136
7 Tinoco, I. and Yamaoko, K. *J. Phys. Chem.* 1959, **63**, 423
8 Benoit, H. *Ann. Phys. 12e Sér.* 1951, **6**, 1
9 O'Konski, C. T., Yoshioka, K. and Orttung, W. H. *J. Am. Chem. Soc.* 1959, **63**, 1558
10 Tsvetkov, V. N., 'Newer Methods of Polymer Characterization, XIV, Flow Birefringence', Ed. K. Bacon, Wiley Interscience Publishers, 1964, pp. 563–665
11 Cerf, R. *C.R. Acad. Sci. Paris*, 1948, **226**, 1586
12 Fijnaut, H. M., Pathmamanoharan, C., Nieuwenhuis, E. A. and Vrij, A. *Chem. Phys. Lett.* 1978, **59**, 351
13 Fijnaut, H. M., Dhont, J. K. G. and Nieuwenhuis, E. A. *Adv. Colloid Interface Sci.* 1982, **16**, 161
14 Fijnaut, H. M. *J. Chem. Phys.* 1981, **74**, 6857
15 Bedeaux, D., Kapral, R. and Mazur, P. *Physica (Utrecht)* 1977, **88A**, 88
16 Lutz, P., *Thesis*, Strasbourg, 1976
17 Guinier, A. and Fournet, D., 'Small Angle X-Ray Scattering', J. Wiley, London, 1955
18 De Gennes, P. G., 'Scaling Concepts in Polymer Physics', Cornell University Press, Ithaca, New York, 1979
19 Benoit, H., Wu, W., Benmouna, M., Mozer, B., Bauer, B. and Lapp, A. *Macromolecules* 1985, **18**, 986
20 Wilkes, C. E., Folt, V. and Krimm, S. *Macromolecules* 1973, **6**, 235
21 Berghmans, H., Govaerts, F. and Ovebegh, N. *J. Polym. Sci., Polym. Phys. Edn.* 1979, **17**, 1251